

# Space-temporal behavior of a light pulse propagating in a nonlinear nondispersive medium

A. Yu. Okulov and A. N. Oraevsky

*P. N. Lebedev Physical Institute, Academy of Sciences of the USSR, Leninsky Prospect 53, 117924 Moscow, USSR*

Received October 8, 1985; accepted November 18, 1985

An analytical method for the calculation of the evolution of a spatially inhomogeneous light pulse in a nonlinear optical system is developed. The description of pulse modulation is derived by using a one-dimensional map with a quadratic maximum that shows regular and chaotic dynamics according to Feigenbaum theory. This mechanism may dominate for a ring laser or a nonhomogeneous medium with alternating amplifying and nonlinear absorbing layers. The total length of the system should be sufficiently small that dispersion and diffraction effects do not appear. In this paper we present two-dimensional distributions of the wave field intensity that illustrate regular and chaotic self-modulation of the light pulse. We give quantitative estimates for such regimes of a ring laser with a saturable absorber, the losses into the harmonics, stimulated scattering, etc. It is found that for period-doubling bifurcations to occur there is no need for total conversion of the pulse into the harmonic or Stokes component.

## INTRODUCTION

Different types of instabilities in nonlinear systems<sup>1</sup> are described by finite-dimensional iterative maps, particularly one-dimensional (1-D) maps with quadratic extrema.<sup>2</sup> Such a map may connect, for example, the amplitudes of oscillations separated by a certain time interval (Poincaré map). It is usually made by the numerical integration of differential equations that correspond to a given nonlinear system. However, in some cases a 1-D map has a clear physical meaning and can be derived analytically, as in a traveling-wave tube generator with delayed feedback<sup>3</sup> or in a ring laser with second-harmonic losses.<sup>4</sup> For the latter case such a laser should perform temporal modulation (with switching time  $\sim 1$  psec) of ultrashort light pulses (see Fig. 1). Self-modulation is due to the discrete nature of the attracting set of the 1-D map, and the most important feature of such an analytical description lies in the possibility of predicting the values of the laser parameters that correspond to regular and chaotic regimes. However, the quantitative consideration in Ref. 4 was restricted by a number of limitations (not always experimentally convenient) such as linear (unsaturated) laser gain, perfect phase matching of harmonics, and the homogeneous transverse profile of the light pulse and of the laser parameters.

Our aim here is to show that the above restrictions are not necessary for an analytical description of nonlinear optical systems by 1-D maps. Furthermore, it is a transverse non-uniformity of the laser beam and the amplifier gain that leads to the most interesting result: spatial self-modulation. As a result, the space-temporal picture of the pulse exhibits a complex structure composed of coexisting regions with regular and chaotic intensity behavior. This behavior is due to period-doubling bifurcations of 1-D maps and differs from the transverse instability reported in Ref. 5. We also discuss sufficient conditions for such a 1-D description, and they prove to be valid not only for the second harmonic but for different types of nonlinear processes as well (including stimulated light scattering).

## ONE-DIMENSIONAL MAPS FOR LIGHT PULSES IN MEDIA WITH LOCAL RESPONSE AND NO DIFFRACTION

The map with the quadratic extremum introduced in Ref. 4 connects the values of the amplitudes of the electric field of the pulse from any trip through the ring laser to the next one. The phase value may be neglected owing to the absence of interference at the entry mirror because of the short pulse duration  $\tau \ll l/c$ , where  $l$  is optical length of the ring laser ( $l = 0.1$ – $1$  m). The above condition is certainly fulfilled for ultrashort pulses ( $\tau \approx 10$ – $100$  psec). One should note here that when taking interference into account it is necessary to use at most a two-dimensional map, because in that case the information about the phase becomes significant.<sup>6</sup>

Suppose that the electric field  $E(t, \mathbf{r}_\perp)$  at a certain moment of time  $t$  and at a point  $\mathbf{r}_\perp$  depends on its value just at the same moment of the previous round trip and at the same point  $\mathbf{r}_\perp$  (see Fig. 1). This assumption could be justified only when the effects of nonlocal response (that is, temporal and spatial dispersion<sup>7</sup>) and diffraction are weak. To be more precise, linear dispersion may be neglected at a small group-velocity mismatch  $d \ll (u_1^{-1} - u_2^{-1})^{-1} \times \delta\tau$  and at a slight dispersion creep  $d \ll (\partial^2 K / \partial \omega^2)^{-1} \times \delta\tau^2 / 2$ , where  $u_1$  and  $u_2$  are group velocities of the interacting waves,  $\delta\tau$  is the effective duration of a spike in the temporal structure of the pulse, and  $d$  is the optical width of the medium. At resonant interaction times  $\delta\tau$  should be longer than at intrinsic relaxation times [for two-level system: longitudinal ( $T_1$ ) and transverse ( $T_2$ ) relaxation times]. One can neglect diffraction if only the Fresnel number is sufficiently large:  $N = [\delta a^2 / (\lambda \times l \times n)] \gg 1$ , where  $\delta a$  is the effective size of spatial inhomogeneity,  $\lambda$  is the wave length,  $l$  is optical length of the laser, and  $n$  is the number of trips.

As soon as the two conditions above (absence of interference and nonlocality) are satisfied, then successive propagation of the pulse through the elements of the ring laser is governed by a 1-D map of the general form

$$I_{n+1}(t, \mathbf{r}_\perp) = Rf[g[I_n(\mathbf{r}_\perp, t)], \mathbf{r}_\perp], \quad (1)$$

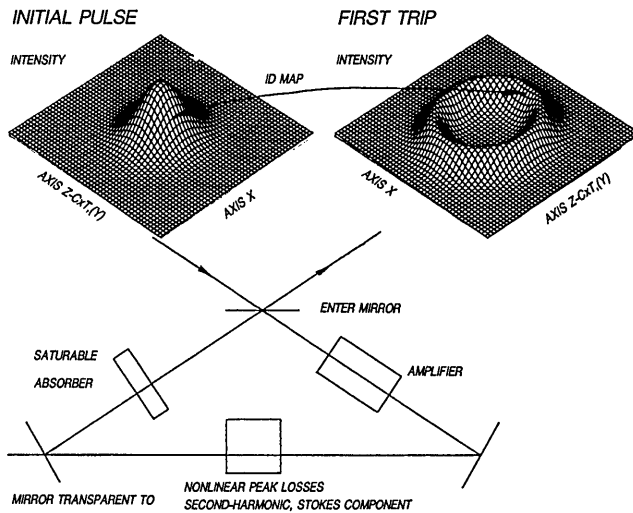


Fig. 1. Ring laser with saturable absorber and nonlinear losses described by 1-D map.

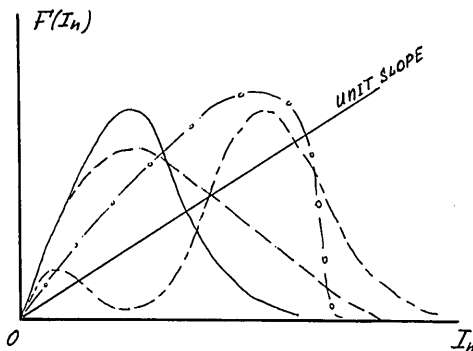


Fig. 2. Diagrams of 1-D maps corresponding to different mechanisms of nonlinear losses: solid line, losses into the second harmonic under phase synchronism; long-dashed line, losses into the third harmonic under the same conditions; dotted-dashed line, stimulated Raman scattering (SRS) with the initial Stokes intensity  $I_S(0) = 10^{-2} \times I_n$ ; long- and short-dashed line, generation of the second harmonic in the absence of phase synchronism  $K = 0.2 \text{ cm}^{-1}$ .

where  $I_n$  is the intensity at  $n$ th trip through the system,  $R$  is the entry-mirror reflection coefficient, and  $g = (I_n)$  is the nonlinear (saturated) gain. Transverse coordinates  $\mathbf{r}_\perp$  describe the spatial inhomogeneity of the light beam or the laser parameters. For a particular system with nonlinear second-harmonic losses<sup>4</sup> the map takes the form

$$I_{n+1} = Rg(I_n)\{1 - th^2[\sigma d \sqrt{g(I_n)}]\}, \quad (2)$$

where  $\sigma$  is the coupling constant between the harmonics. The physical meaning of this map is clear: The first term describes the gain; the second, nonlinear losses, i.e., conversion into the second harmonic (see Fig. 2). We shall note now that the type of map will not differ qualitatively from the one shown in Ref. 4; if the gain is nonlinear, the conversion is performed in the absence of phase synchronism or into other harmonics. It is sufficient if the losses significantly exceed the amplification at a certain intensity value. For example, for third-harmonic losses under phase synchronism we have

$$I_{n+1} = Rg(I_n)/[1 + \sigma^2 d^2 g^2(I_n)], \quad (3)$$

and for the second-harmonic losses in the absence of phase synchronism ( $\Delta K = 2 \times K_1 - K_2 \neq 0$ ) we have<sup>8</sup>

$$I_{n+1} = Rg(I_n)\{1 - aSn^2[\sigma d \sqrt{g(I_n)}/\sqrt{a}, 1 - a^2]\},$$

$$a = \left(2 + \frac{\Delta S^2}{4} + \sqrt{\frac{\Delta S^4}{16} + \frac{\Delta S^2}{4}}\right)/2;$$

$$\Delta S = \Delta K/[\sigma g(I_n)], \quad (4)$$

where  $K_{1,2}$  are the wave numbers of the first and second harmonics, respectively, and  $Sn$  is the Jacobi elliptic sine.

The conditions for validity of the maps [Eqs. (2)–(4)] are provided by choosing the nonlinear medium. For a KDP crystal with  $d = 1 \text{ cm}$ ,  $\lambda = 1.06 \mu\text{m}$ ,  $\delta\tau = 10\text{--}100 \text{ psec}$ , the coherent length due to the dispersion of group velocities is  $\delta\tau(u_1^{-1} - u_2^{-1})^{-1} \approx 75\text{--}750 \text{ cm} \gg d$ ,<sup>9</sup> and the one due to dispersion creep<sup>9</sup> is  $(\delta\tau/2)(\partial^2 K/\partial\omega^2)^{-1} \approx 10^3 \text{ cm}$ . The inertia of the electronic nonlinearity at such durations is insignificant.<sup>10</sup>

Another mechanism for nonlinear losses may be stimulated Raman scattering (SRS). Consider the case when the pump wave and the Stokes wave are propagating in the same direction. For a steady-state limit the relation between the Stokes wave intensity  $I_S$  and the pump intensity  $I_p(0)$  is given by the integration of equations for nonlinear SRS<sup>8</sup>:

$$I_S = \frac{[I_p(0) + I_S(0)]I_S(0)}{(I_p(0) * \exp[-I_p(0) + I_S(0)]\sigma d + I_S(0))},$$

where  $\sigma$  is the coupling constant of the Stokes wave and the pump wave,  $d$  is the medium thickness, and  $I_p(0)$ ,  $I_S(0)$  is the intensity at the entry. For generation from spontaneous noise to occur the increment should be 20–30. Hence the intensity is 200–300 MW/cm<sup>2</sup> for a medium 10 cm long, provided that the coupling constant is  $\sigma \approx 10^{-2} \text{ cm/MW}$  (CS<sub>2</sub>).<sup>11</sup> The condition for a steady state lies in neglecting the inertia of the molecular vibrations ( $T_2 \approx 10 \text{ psec}$ ) and the dispersion of group velocities of pump and Stokes waves; the coherent length is  $\approx 10^3 \text{ cm}$  for  $\delta\tau \approx 10 \text{ psec}$  according to Ref. 12. Considering the trip of the pulse through the amplifier  $g[I_n(t)]$ , the Raman converter, and the entry mirror  $R$ , under such conditions one may easily obtain the following 1-D map:

$$I_{n+1} = \frac{R[g(I_n) + I_S(0)]g(I_n)}{I_S(0)\exp\{\sigma d[g(I_n) + I_S(0)]\} + g(I_n)}. \quad (5)$$

One more source of nonlinear losses is the saturable absorber. In the instantaneous response limit<sup>13</sup> the rate equations for the two-level medium<sup>14</sup> are easily integrated, and they give the relation between the entry  $g[I_n(t)]$  and the exit  $I_{n+1}(t)$  intensities through the following transcendental equation:

$$\frac{I_{n+1}}{R} \exp\left(\sigma_{\text{abs}} T_{1\text{abs}} \frac{I_{n+1}}{R}\right) = \frac{\exp[\sigma_{\text{abs}} T_{1\text{abs}} g(I_n)]g(I_n)}{\exp[\sigma_{\text{abs}} N_{\text{abs}} d_{\text{abs}}]}, \quad (6)$$

where  $\sigma_{\text{abs}}$  is the cross section of the saturable absorption,  $N_{\text{abs}}$  is the concentration of the absorbing particles per unit volume, and  $d_{\text{abs}}$  is the absorber thickness.

The equation for nonlinear gain  $g(I_n)$  is analogous:

$$g(I_n)\exp[\sigma_{\text{amp}} T_{\text{amp}} g(I_n)] = \exp[\sigma_{\text{amp}} T_{1\text{amp}} g(I_n)]\exp[\sigma_{\text{amp}} N_{\text{amp}} d_{\text{amp}}]I_n. \quad (7)$$

This equation differs from Eq. (6) only in the sign of the active particles' concentration  $N_{amp}$ , and this corresponds to the amplifying medium, not to the absorbing one. This integration procedure is justified only when  $\delta\tau$  is longer than  $T_1$  and  $T_2$  and the group delay  $(d_{abs,amp}/c) < \delta\tau$ . The more complicated case of noninstantaneous response and significant diffraction has been considered to some extent in recent papers.<sup>15</sup>

**MODULATION PROPERTIES OF ONE-DIMENSIONAL MAPS**

Let us now consider the modulation properties of the maps [Eqs. (2)–(7)]. Begin with the last two, as this enables us to make a comparison with the known results for a two-component laser medium having instantaneous response in the case when

$$\sigma_{abs} T_{1abs} > \sigma_{amp} T_{1amp}, \quad \sigma_{abs} N_{abs} d_{abs} > \sigma_{amp} N_{amp} d_{amp} \quad (8)$$

Figures 3(a) and 3(b) show diagrams of the maps given by Eqs. (6) and (7), respectively. They demonstrate linear absorption (amplification) at small intensities and the saturation that leads to free passage of large intensities through the medium. The sum action of the saturable absorption and amplification is described by the map presented in Fig. 3(c).

Since we assumed above that the absorbing medium is saturated before the amplifying one [Eq. (8)], then (1) at small intensities absorption dominates, (2) at moderate intensities amplification prevails, and (3) at high intensities the amplifier is saturated and the input mirror's and other nonresonant losses are left. As can be seen from Fig. 3(c), the line with the unit slope doubly intersects the diagram of the sum map. Both points of intersection correspond to the fixed points of this map. The lower point  $I_{thr}$  is unstable, as  $|dI_{n+1}/dI_n| = R \exp(\sigma_{amp} N_{amp} d_{amp}) > 1$ . This means<sup>2</sup> that the values of  $I$  smaller than  $I_{thr}$  under successive mapping come to zero, and the values larger than  $I_{thr}$  are growing. The same conclusion was reached in Ref. 14, where it was noted that a two-component laser medium is a threshold element that is transparent to light spikes of intensity higher than  $I_{thr}$ . In Ref. 16 this property of the two-component medium was used to single out and amplify a separate burst inside the temporal structure of an ultrashort pulse.

Now we show that such a burst becomes rectangular under the action of a 1-D map [see Fig. 3(c)]. Consider the second stationary point  $I_{sta}$ . According to Ref. 2 it is stationary because here  $|dI_{n+1}/dI_n| = R < 1$ . Because there are no other stationary points, this means that all the values  $I_n(t)$  higher than the threshold  $I_{thr}$  tend to  $I_{sta}$ . Consequently, the pulse envelope should tend to be rectangular under the action of the saturable nonlinearities. This will, obviously, take place until the influence of dispersive elements is apparent. The presence of such elements, as proved in Ref. 17, leads to smoothing of the pulse fronts.

Consider now the regime when  $I_{sta}$  loses its stability. This is possible for  $|dI_{n+1}/dI_n| > 1$ , which occurs in the case of Eqs. (2), (4), and (5). [For Eq. (3)  $|dI_{n+1}/dI_n| < 1$  and  $I_{sta}$  is always stable.] Then, as is shown in Ref. 2, three stationary points appear in two successive iterations:  $I_{n+2} = f[f(I_n)]$ . Two of these points are stable (under moderate values of the

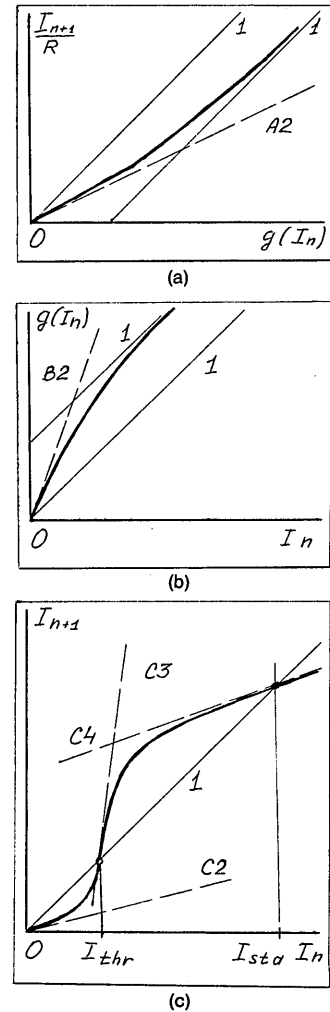


Fig. 3. Diagrams of the maps for two-component laser medium with saturation on intensity. Solid lines numbered 1 have a unit slope. Dashed lines are asymptotes, to which the graphs of the maps (solid curves) tend at different intensities  $I_n$ . The asymptotes have the following slopes: A2,  $d(I_{n+1}/R)/dg(I_n) = \exp(-G_{abs}) < 1$ ; B2,  $dg(I_n)/dI_n = \exp(G_{amp}) > 1$ ; C2,  $dI_{n+1}/dI_n = R \times \exp(G_{amp} - G_{abs}) < 1$  [for details see Eq. (8)]; C3,  $dI_{n+1}/dI_n = R \times \exp(G_{amp}) > 1$  (unsaturated gain and saturated absorption); C4,  $dI_{n+1}/dI_n = R < 1$  (gain and absorption saturated).  $G_{abs} = \sigma_{abs} \times N_{abs} \times d_{abs}$ ,  $G_{amp} = \sigma_{amp} \times N_{amp} \times d_{amp}$ .

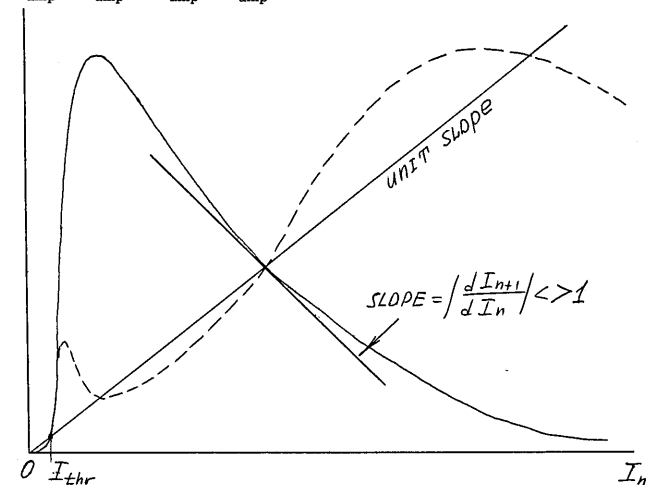


Fig. 4. 1-D map with quadratic extremum exhibits the loss of stability of fixed point  $I$  when gain  $G$  is sufficiently large. Solid curve,  $I_{n+1} = f(I_n)$ ; dashed curve,  $I_{n+2} = f[f(I_n)]$ .

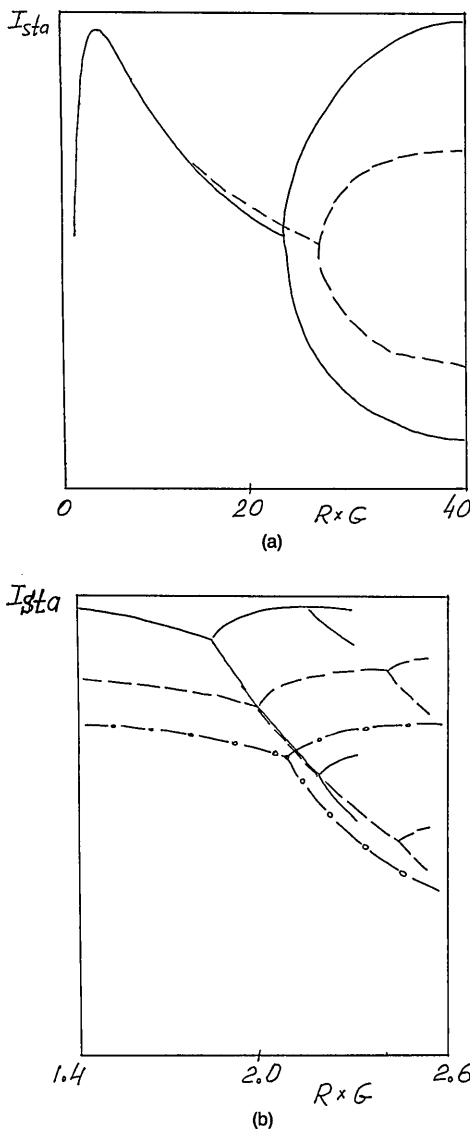


Fig. 5. Dependence of stable fixed-point values on the critical parameter. (a) Second-harmonic generation with phase detuning  $\Delta K = 0$  (solid line) and  $\Delta K = 0.2 \text{ cm}^{-1}$  (dashed line). (b) SRS with initial Stokes intensity  $I_S(0) = 10^{-2} I_n$ . Solid lines,  $I_S(0) = 5 \times 10^{-3} I_p(0)$ ; dashed lines,  $I_S(0) = 10^{-2} I_p(0)$ ; dotted-dashed lines,  $I_S(0) = 1.5 \times 10^{-2} I_p(0)$ .

critical parameter  $\kappa = GR$  (see Fig. 4). According to Ref. 4, this corresponds to the reconstruction of the pulse form  $I_n(t)$  after two round trips through the system. With a further increase in the critical parameter successive doubling of the states occurs according to the known quantitative laws.<sup>2</sup>

Consider the peculiarities of such doubling for the maps in Eqs. (2), (4), and (5). First, the calculation of  $\delta$  by the values  $\kappa_m$  for the first bifurcations gives values considerably different from  $4.669 \dots$ , i.e., the rate of convergence of  $(\kappa_{m+1} - \kappa_m)/(\kappa_{m+2} - \kappa_{m+1})$ ,  $m \rightarrow \infty$  is not so high as the one for a logistic map.<sup>2</sup> Second, the values  $\kappa_m$  for Eqs. (2), (4), and (5) differ markedly and show dependence on the parameters of the maps. So for Eq. (4) one may observe the modification of the bifurcation diagram by increasing the phase detuning  $\Delta K = 0-0.2 \text{ cm}^{-1}$ . Figure 5(a) shows the growth of the bifurcation values  $\kappa_1$  and  $\kappa_2$ . This is connected with the fact that at the second fixed point (see Fig. 4) the modulus of the

derivative drops with the growth of  $\Delta K$ . As a result, it loses its stability at higher values of  $\kappa = GR$ . The behavior of the bifurcation diagram in Fig. 5(b) is governed by an analogous mechanism. This diagram demonstrates bifurcations of Eq. (5) at different intensities of the entry Stokes signal  $I_S(0)$ .

### SPACE-TEMPORAL SELF-MODULATION

We have considered different variants of the map [Eq. (1)] without taking into account the dependencies of the intensity and the parameters of the system (e.g.,  $G$ ,  $\Delta$ , and  $K$ ) on the transverse coordinates  $\mathbf{r}_\perp$ . We now show that taking this dependence into account results, even within the framework of applicability of the map [Eq. (1)], in a highly complex evolution of the pulse envelope. Consider the propagation of a two-dimensional Gaussian pulse [Fig. 6(a)]. The figure shows the dependence of the intensity on the time  $(t - z/c)$  and the transverse coordinate  $x$ . Dependence only on the transverse coordinate  $x$  corresponds to cylindrical geometry, in which the distribution over the  $y$  axis is practically homogeneous. One may analogously depict the dependence only on the space coordinates  $x$  and  $y$  at a determined moment of time.

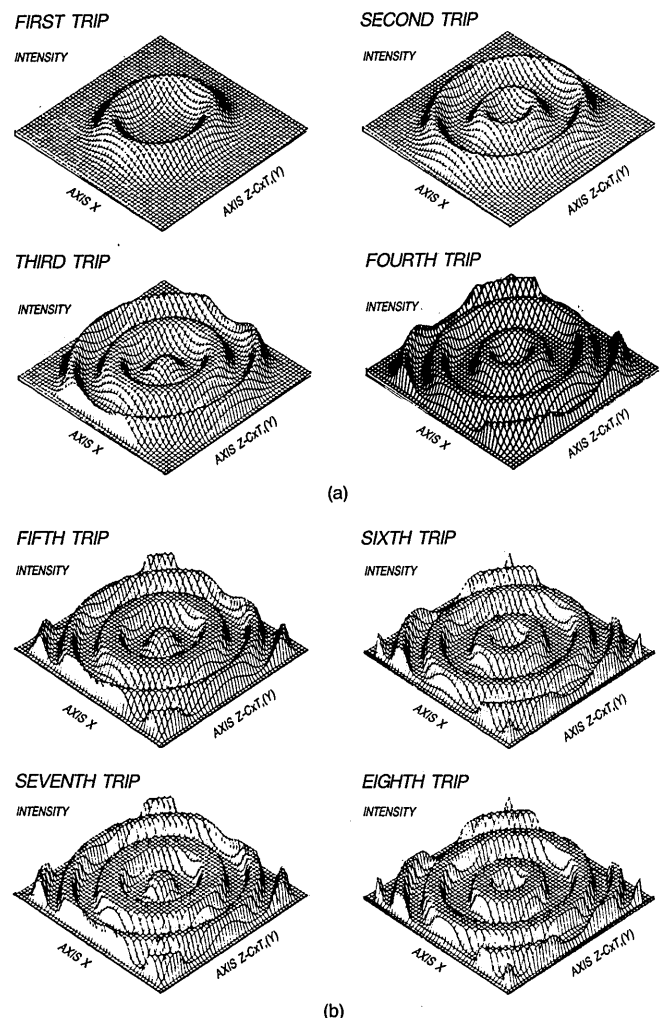


Fig. 6. Evolution of space-temporal structure of the pulse at different numbers of round trips through the system ( $GR = 26$ ).

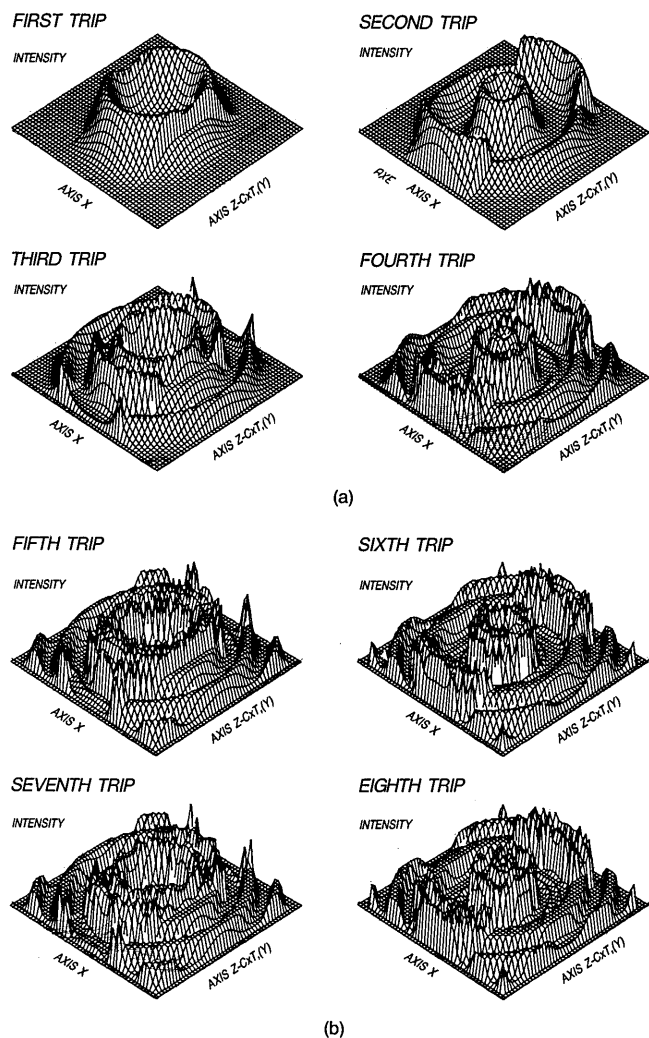


Fig. 7. Same as Fig. 6 but presented for inhomogeneous rectangular distribution of the gain coefficient  $G$  over the pulse cross section: in the center  $GR = 56$ ; at the sides  $GR = 26$ .

Consider what happens to the envelope of such a Gaussian pulse under the action of a nonlinear, nondispersive transformation [Eq. (1) = Eqs. (2) + (6) + (7)] for  $GR = 26$  (two-level modulation). Remember that the use of such a map corresponds to pulse propagation in a ring laser with a saturable absorber and conversion into the second harmonic under the phase synchronism. The use of the absorber results in the damping of intensities lower than  $I_{thr}$ . Thus the pulses presented in Figs. 6 and 7 are limited in space and time as well.

Figure 6(a) illustrates that after one round trip the intensity drops at the points with relatively high initial intensity owing to considerable losses into the harmonic. At the same time, at the points with small intensity, losses into the harmonic are insignificant, and the intensity grows because of the amplification. In further round trips the intensity values tend to be stable, fixed points (modulation levels) [see Figs. 6(a) and 6(b)]. The circular symmetry of the pattern is determined by the symmetry of the initial Gaussian pulse (see Fig. 1). After eight round trips [Fig. 6(b)] a typical structure is formed that has almost plane tops and bottoms. Here, because of the nondispersive character of the 1-D

map,<sup>4</sup> a noticeable steepening of the envelope is observed. It should be noted that such space-temporal self-modulation limits the applicability of the point map. This is explained (see Fig. 6) by the decrease in the typical size of the space inhomogeneity of the pulse, and, as a consequence, of the Fresnel number  $N = \delta a^2 / (\lambda l n)$  as well.

The behavior of the pulse under the high critical parameter  $GR$  is illustrated by Fig. 7. After the first two round trips the shape of the envelope does not differ qualitatively from that of two-level modulation, while absolute values of the intensity in the maxima are somewhat higher. In further round trips the presence of a larger number of the modulation levels becomes apparent. In the example given, the number of levels in the central part of the pulse is infinite, and it corresponds to the chaotic modulation ( $GR = 56$ ). As a result, up to the eighth round trip [Fig. 7(b)] the envelope is close to irregular, and it is characterized by a considerable number of bursts of different amplitudes. At the same time, at the sides a regular structure is formed that is analogous to the one shown in Fig. 6(b) with two modulation levels (here  $GR = 26$ ). The example in Fig. 7 shows that a simple description of the evolution of the laser pulse by a 1-D map with the parameters dependent on transverse coordinates leads to outwardly complex space-temporal dynamics.

## CONCLUSION

Consider now for which laser systems a 1-D description will be correct. Without restricting ourselves only to the ring-laser system we can say that the most common model of such a system could be presented by a sequence of alternating elements with amplification and elements with nonlinear losses. The total length of the system should be sufficiently short: It is the case that the dispersion and diffraction are negligible. A typical example of such a system was considered in Ref. 18.

For period-doubling bifurcations to occur there is no need for total conversion of the light pulse into optical harmonics or Raman components [Eqs. (2)–(5)]. In other words, the diagrams of the maps should not tend to zero at large intensities, because it is sufficient that  $|dI_{n+1}/dI_n| > 1$  at fixed points of the maps. For example, the diagram of the map of Eq. (4) oscillates, intersecting the line with a unit slope many times (Fig. 2 shows two such oscillations). Nevertheless, the period-doubling bifurcations still occur, and at a certain value  $GR$  they lead to chaotic motion. At the same time, the second-harmonic efficiency at the pulse maximum is  $\approx 80\%$  ( $\Delta K = 0.2 \text{ cm}^{-1}$ ), while the energy efficiency is considerably smaller. Therefore practical realization of such period-doubling regimes seems to be more likely. The above consideration indicates that it may be possible to observe instabilities of the space-temporal structure of the light pulse discussed just now. Of course, 1-D approximation gives a rough picture of such instabilities, and satisfactory agreement between theory and experiment could be obtained only by taking into account the nonlocal effects, i.e., dispersion and diffraction. An interesting approach was proposed in Ref. 15, where an attempt was made to include nonlocality directly in the discrete dynamics without solving the whole set of partial differential equations. We hope to consider some aspects of this approach in future work.

## ACKNOWLEDGMENT

The authors are grateful to P. G. Kryukov for valuable discussions.

## REFERENCES

1. E. N. Lorenz, *J. Atmos. Sci.* **20**, 130 (1963); A. Z. Grasyuk and A. N. Oraevsky, *Radio Eng. Electron. Phys. (USSR)* **9**, 924 (1964).
2. M. J. Feigenbaum, *J. Stat. Phys.* **19**, 25 (1978).
3. Yu. M. Azyan and V. V. Migulin, *Radiotekh. Elektron.* **1**, 418 (1956); V. Ya. Kislov, *Radiotekh. Elektron.* **25**, 1683 (1980).
4. A. Yu. Okulov and A. N. Oraevsky, *Kvantovaya Elektron.* **11**, 1844 (1984).
5. D. W. McLaughlin, J. V. Moloney, and A. C. Newell, *Phys. Rev. Lett.* **54**, 681 (1985).
6. H. Nakatsuka, S. Asaka, H. Itoh, K. Ikeda, and M. Matsuoka, *Phys. Rev. Lett.* **50**, 109 (1983).
7. L. D. Landau and E. M. Lifshits, *Elektrodinamika Sploshnykh Sred (Electrodynamics of Solid Media)* (Nauka, Moscow, 1982).
8. N. Blombergen, in *Nonlinear Optics*, A. S. Akhmanov and R. V. Khokhlov, eds. (Mir, Moscow, 1966).
9. A. M. Prokhorov, ed., *Handbook of Lasers* (Soviet Radio, Moscow, 1978), p. 315.
10. I. Yu. Pirogova and A. P. Sukhorukov, *Opt. Spektrosk.* **59**, 694 (1985).
11. M. Maier, W. Kaiser, and J. A. Giordmaine, *Phys. Rev.* **177**, 580 (1969).
12. G. P. Dzhotyan, Yu. E. Dyakov, I. G. Zubarev, A. B. Mironov, and S. I. Mikhailov, *Zh. Eksp. Teor. Fiz.* **73**, 822 (1977).
13. M. A. Vasil'eva, V. B. Gul'binas, V. I. Kabelka, A. V. Masalov, and V. P. Syrus, *Kvantovaya Elektron.* **10**, 415 (1983).
14. P. G. Kryukov and V. S. Letokhov, *Usp. Fiz. Nauk* **99**, 169 (1969).
15. F. Hollinger and C. Jung, *J. Opt. Soc. Am. B* **2**, 218 (1985); D. Yu. Kuznetsov and T. I. Kuznetsova, *Kvantovaya Elektron.* **12**, 2507 (1985).
16. P. G. Kryukov, Yu. A. Matveets, S. V. Chekalin, and O. B. Shatberashvili, *Pi'sma Zh. Eksp. Teor. Fiz.* **16**, 177 (1972).
17. H. A. Haus, *IEEE J. Quantum Electron.* **QE-11**, 736 (1975); P. P. Vasil'ev and V. N. Morozov, *Kvantovaya Elektron.* **12**, 331 (1985).
18. N. E. Bykovsky and Yu. V. Senatsky, Preprint No. 15 (P. N. Lebedev Physical Institute, Moscow, 1977).